Title	Para-equilibrium phase diagrams
Author(s)	Pelton, Arthur D.; Koukkari, Pertti; Pajarre, Risto; Eriksson, Gunnar
Citation	Journal of Chemical Thermodynamics . Elsevier . Vol. 72 (2014) No: May, pages 16-22
Date	2014
URL	http://dx.doi.org/10.1016/j.jct.2013.12.023
Rights	Manuscript version of the article. This article may be downloaded for personal use only.

Paraequilibrium phase diagrams

Arthur D. Pelton[a], Pertti Koukkari[b], Risto Pajarre[b] and Gunnar Eriksson[c]

[a] *Corresponding author,*
CRCT - Centre de Recherche en Calcul Thermochimique, Dép. de génie chimique, École Polytechnique, C.P. 6079, Succ.Centre Ville, Montréal, Québec H3C 3A7, Canada,
tel: 1-514-340-4711(ext 4531), fax: 1-514-340-5840, e-mail : apelton@polymtl.ca
[b] *VTT Technical Research Centre of Finland, P.O. Box 1000, FI-02044 VTT, Finland*
[c] *GTT- Technologies, Kaiserstrasse 100, D-52134 Herzogenrath, Germany*

ABSTRACT

If an initially homogeneous system at high temperature is rapidly cooled, a temporary paraequilibrium state may result in which rapidly diffusing elements have reached equilibrium but more slowly diffusing elements have remained essentially immobile. The best known example occurs when homogeneous austenite is quenched. A paraequilibrium phase assemblage may be calculated thermodynamically by Gibbs energy minimization under the constraint that the ratios of the slowly diffusing elements are the same in all phases. Several examples of calculated paraequilibrium phase diagram sections are presented and the application of the Phase Rule is discussed. Although the rules governing the geometry of these diagrams may appear at first to be somewhat different from those for full equilibrium phase diagrams, it is shown that in fact they obey exactly the same rules with the following provision. Since the molar ratios of non-diffusing elements are the same in all phases at paraequilibrium, these ratios act, as far as the geometry of the diagram is concerned, like "potential" variables (such as T, pressure or chemical potentials) rather than like "normal" composition variables which need not be the same in all phases. A general algorithm to calculate paraequilibrium phase diagrams is presented. In the limit, if a paraequilibrium calculation is performed under the constraint that no elements diffuse, then the resultant phase diagram shows the single phase with the minimum Gibbs energy at any point on the diagram; such calculations are of interest in physical vapour deposition when deposition is so rapid that phase separation does not occur.

Keywords: Paraequilibrium, phase diagrams, thermodynamics, Phase Rule, physical vapour deposition

1. Introduction

In certain solid systems, some elements diffuse much faster than others. Hence, if an initially homogeneous single-phase system at high temperature is rapidly cooled and then held at a lower temperature, a temporary paraequilibrium state may result in which the rapidly diffusing elements have reached equilibrium but the more slowly diffusing elements have remained essentially immobile [1-3]. The best known and most industrially important example occurs when homogeneous austenite is quenched and annealed; interstitial elements such as C and N are much more mobile than the metallic elements. Of course, in reality some diffusion of the metallic elements will always occur [2], so that paraequilibrium is a limiting state which is never

fully realized but may, nevertheless, be reasonably closely approached in many cases.

The present article discusses the thermodynamic calculation of paraequilibrium and paraequilibrium phase diagrams and the geometrical rules governing the latter (that is, the application of the Phase Rule to paraequilibrium phase diagrams.)

The FactSage 6.4 thermodynamic software [4] calculates the conditions for full thermodynamic equilibrium (sometimes called orthoequilibrium) by Gibbs energy minimization, taking data from databases which contain optimized thermodynamic model parameters giving the Gibbs energy of all phases as functions of temperature and composition. These model parameters have been obtained by critical evaluation of literature data. The FactSage thermodynamic software can calculate and plot equilibrium phase diagrams through the repeated systematic application of the Gibbs energy minimization algorithm.

At paraequilibrium, the ratios of the slowly diffusing elements are the same in all phases and are equal to their ratios in the initial single-phase high-temperature alloy. Hence, the calculation of paraequilibrium simply involves modifying the Gibbs energy minimization algorithm by the addition of this constraint. This will be discussed in detail in Section 5. Paraequilibrium phase diagram sections can subsequently be calculated by exactly the same procedure as is used to calculate full equilibrium phase diagrams as will be discussed in Section 4.

In the limit, if a paraequilibrium calculation is performed under the constraint that no elements diffuse, then the ratios of all elements remain the same as in the initial homogeneous high-temperature state. Hence, such a calculation will simply yield the single homogeneous phase with the minimum Gibbs energy at the temperature and overall composition of the calculation. Such calculations are of practical interest in physical vapour deposition (PVD) when deposition from the vapour phase is so rapid that phase separation does not occur, resulting in a single-phase solid deposit. The calculation of minimum Gibbs energy phase diagrams will be discussed in Section 3.

In the following section, the application of the Phase rule to paraequilibrium phase diagrams is discussed.

2. The geometry of paraequilibrium phase diagram sections

All figures shown in this article were calculated with the FactSage 6.4 software [4], with thermodynamic data taken from the FactSage FSstel steel database. In all calculations the formation of graphite has been suppressed.

In the Fe-Cr-C system at elevated temperatures the range of homogeneous austenite (FCC) extends from pure Fe to approximately 8 mol % C and 15 mol % Cr as can be seen in the (full orthoequilibrium) isothermal phase diagram section at 1140^{o}C in figure 1. Alloys with compositions in this range, when cooled rapidly and then held at a lower temperature, may exhibit a temporary paraequilibrium state. A vertical section of the same (full orthoequilibrium) Fe-Cr-C phase diagram section is shown in figure 2 where the molar ratio C/(Fe+Cr) is plotted

versus temperature, *T*, at a constant molar metal ratio Cr/(Fe+Cr) = 0.04. (On figures 1 and 2 and other figures, $M_{23}C_6$, M_7C_3 and Cementite are solutions of Fe and Cr carbides.)

Before discussing the geometry of paraequilibrium phase diagrams, we should recall the Law of Adjoining Phase Regions (LAPR) [5-7] which applies to all single-valued phase diagram sections: "As a phase boundary line is crossed, one and only one phase either appears or disappears." (In phase diagrams involving axes other than temperature and composition, such as pressure, volume and chemical potential, it is possible to define the axes in such a way that the diagram is not single-valued in every region. In this case the LAPR does not apply in these regions [6,7]. However, diagrams with temperature and composition as axes are always single-valued and the LAPR always applies.) An examination of figures 1 and 2 will show that the LAPR applies to every phase boundary. Although the isothermal lines *abc* and *def* in figure 2 might, at first, appear to be exceptions to the rule, these lines are not simple phase boundaries but are, rather, infinitely narrow four-phase fields with coincident upper and lower phase boundaries. For example, the line *abc* is an infinitely narrow (FCC + BCC + M_7C_3 + Cementite) field where the four phases co-exist. Hence, the LAPR applies. The Phase Rule, at constant total pressure, may be written:

$$F = C - P + 1 \qquad (1)$$

where C = number of components, P = number of phases and F = number of degrees of freedom (variance.) In the three-component Fe-Cr-C system when four phases are at equilibrium, $F = 0$. Hence, the line *abc* represents an invariant equilibrium which occurs at only one temperature.

Since a paraequilibrium calculation simply involves an additional constraint, the LAPR also applies to paraequilibrium phase diagram sections.

In figure 3 is shown the paraequilibrium phase diagram for exactly the same section as in figure 2, calculated for the case where C is the only diffusing element. Since the molar ratio Cr/(Fe+Cr) = 0.04 is now constant and the same in every phase, the diagram in this particular example resembles a full (ortho) equilibrium *T*-composition phase diagram of a two-component system, the "components" being $Fe_{0.96}Cr_{0.04}$ and C. The three-phase (FCC + BCC + Cementite) region *bcd* now appears as an isothermal invariant, similar to a binary eutectoid.

The x-axis in figure 3 is the molar ratio C/(Fe+Cr), not the carbon mole fraction X_C = C/(Fe+Cr +C). Similarly, the diagram is calculated at constant ratio Cr/(Fe+Cr), not at constant Cr mole fraction X_{Cr} = Cr/(Fe+Cr+C). If the diagram is recalculated at constant X_{Cr} = 0.04 with the x-axis as X_C, it will be nearly identical to figure 3 since the C content is very small. However, the three-phase region will no longer be isothermal because now the ratio of the non-diffusing elements Cr/(Fe+Cr) varies with X_C and so the diagram can no longer be considered to be that of a pseudo-binary system. This T-X_C paraequilibrium diagram at constant X_{Cr} is plotted in figure 4 where the temperature axis has been greatly expanded to show clearly that the three-phase field is not isothermal. Note, however, that the three-phase field is still infinitely narrow. At any value of X_C the molar ratio Cr/(Fe+Cr) has a fixed value which must be the same in every phase. This additional constraint removes a degree of freedom so that, for the three-phase paraequilibrium, $F = 0$. In other words, at any given X_C there is only one temperature where the

three phases can co-exist, but this temperature varies with X_C.

The LAPR clearly applies to both figures 3 and 4 as, indeed, it does to all paraequilibrium phase diagram sections.

Another isothermal paraequilibrium phase diagram section of the Fe-Cr-C system is shown in figure 5 where the molar ratio Cr/(Fe+Cr) is plotted versus the molar ratio C/(Fe+Cr) at constant $T = 775^oC$. Tie-lines are horizontal in this diagram since all phases at paraequilibrium have the same Cr/(Fe+Cr) ratio. Since this ratio is the same in all phases, it acts, as far as the geometry of the diagrams is concerned, like a "potential variable" (such as *T*, pressure or chemical potential) which is the same in all phases at equilibrium, rather than like a normal composition variable which, in general, is not the same in phases at equilibrium. Indeed, figure 5 clearly has the same topology as a binary *T*-composition full equilibrium phase diagram. When the ratios C/(Fe+Cr) and Cr/(Fe+Cr) are replaced by X_C = C/(Fe+Cr+C) and X_{Cr} = Cr/(Fe+Cr+C) respectively, the diagram of figure 6 results. The tie-lines and the invariant lines are no longer horizontal, but lie along loci of constant Cr/(Fe+Cr) ratio. However, the three-phase fields are still infinitely narrow and, of course, the LAPR applies.

Yet another section of the paraequilibrium phase diagram of the Fe-Cr-C system is shown in figure 7. At a constant molar ratio C/(Fe+Cr) = 0.05, temperature is plotted versus the molar ratio Cr/(Fe+Cr). Both axis variables, *T* and Cr/(Fe+Cr), are the same in all phases at paraequilibrium. That is, as just stated, the ratio Cr/(Fe+Cr) acts like a "potential variable." From the Phase Rule, Eq. (1), when three phases are at equilibrium at constant pressure $F = 3–3+1 = 1$. Hence, the three-phase fields which separate the two-phase fields in figure 7 are infinitely narrow univariant lines. The molar ratio C/(Fe+Cr) is a "normal" composition variable which need not be the same in all phases at equilibrium. Hence, keeping this ratio constant does not decrease the number of degrees of freedom. Note that the lines on figure 7 separating the FCC field from the (FCC + Cementite) and (FCC + $M_{23}C_6$) fields are not infinitely narrow three-phase univariant lines but, rather, are simple phase boundaries. The point in figure 7 where the four univariant lines converge is an infinitely small four-phase invariant field. The LAPR applies.

Figure 8 is a paraequilibrium phase diagram section for the four-component Fe-Cr-C-N system for the case when both C and N, but not Fe or Cr, diffuse. Temperature is plotted versus the molar ratio Cr/(Fe+Cr) with the two composition variable C/(Fe+Cr) and N/(Fe+Cr) constant. From the Phase Rule, Eq. (1), when four phases are at equilibrium, $F = 4\text{-}4+1 = 0$. Hence, four-phase fields appear as infinitely narrow univariant lines. On figure 8 the four-phase univariant regions are the (FCC + BCC + Cementite + $M_{23}C_6$) and (FCC + BCC + Cementite + M_2(C,N)) lines. The other lines on figure 8 are simple phase boundaries.

Figure 9 is a paraequilibrium diagram for the six-component Fe-Cr-Ni-Mn-Mo-C system where C is the only diffusing element. Temperature is plotted versus the "normal" composition variable C/Z, where Z = (Fe+Cr+Ni+Mn+Mo), with the four molar ratios of non-diffusing elements, Cr/Z, Ni/Z, Mn/Z and Mo/Z held constant. Since these ratios are the same in all phases at paraequilibrium, they act like potential variables. Hence, keeping each of these ratios constant removes one degree of freedom. Therefore, for a three-phase equilibrium in this six-

component system, F = 6-3+1-(4) = 0. The three-phase (FCC + BCC + Cementite) region thus appears as an invariant horizontal line in figure 9. The topology of figure 9 is clearly the same as that of figure 3.

For the five-component paraequilibrium phase diagram in figure 10, where C is the only diffusing element, T is plotted versus the "potential" variable Cr/Z, where Z = (Fe + Cr + Ni + Mn), with the "normal" composition variable C/Z and the two "potential" variables Ni/Z and Mn/Z held constant. Hence, three-phase equilibria appear as univariant lines (where F = 5-3+1-(2) = 1) and four-phase equilibria appear as invariant points. The topology of figure 10 is clearly the same as that of figure 7.

2.1 Summary

The rules governing the geometry of full orthoequilibrium phase diagram sections are described in detail in references [6,7]. From the preceding examples it can be seen that paraequilibrium phase diagram sections obey exactly the same rules with the following provision. Since the molar ratios of non-diffusing elements are the same in all phases at paraequilibrium, these ratios act, as far as the geometry of the diagram is concerned, like "potential" variables (such as T, pressure or chemical potentials) rather than like "normal" composition variables which need not be the same in all phases. Furthermore, and for the same reason, holding a ratio of non-diffusing elements constant decreases the number of degrees of freedom of the system by 1.0 (whereas holding a "normal" composition variable does not.)

In the present article, all compositions are expressed as molar ratios. However, replacing molar ratios by mass ratios will, of course, have no effect on the topology of the diagrams.

3. Minimum Gibbs energy phase diagrams

As discussed in Section 1, if a paraequilibrium calculation is performed under the constraint that no elements diffuse, then the ratios of all elements remain the same as in the initial homogeneous high-temperature state. Hence, such a calculation will simply yield the single homogeneous phase with the minimum Gibbs energy at the temperature and overall composition of the calculation. Such calculations are of practical interest in physical vapour deposition (PVD) when deposition from the vapour phase is so rapid that phase separation does not occur, resulting in a single-phase solid deposit.

The full (ortho) equilibrium phase diagram of the Ni-Cr system is shown in figure 11. The corresponding minimum Gibbs energy diagram is shown in figure 12. Clearly, two-phase fields appear as univariant lines. These lines are the loci of the intersections of the curves of Gibbs energy versus composition and are sometimes called T^o lines. Each T^o line in figure 12 lies within the corresponding two-phase region in figure 11.

As can be seen in figure 12, at lower temperatures the sigma phase is the phase with the lowest Gibbs energy in alloys containing approximately 63 to 73 % Cr, even though this phase does not

appear in the equilibrium phase diagram. This was pointed out previously by Saunders and Miodownik [8] and Spencer [9] who noted that sigma deposits have been observed in vapour-deposited Ni-Cr samples over this approximate composition range at 25^{o}C.

Another example of a calculated minimum Gibbs energy phase diagram is shown in figure 13.

Clearly, minimum Gibbs energy phase diagrams obey the geometrical rules enumerated in Section 2.1.

4. Procedure for calculating paraequilibrium phase diagram sections

Since, as has been demonstrated, paraequilibrium phase diagram sections obey exactly the same geometrical rules as full (ortho) equilibrium diagrams, they can be calculated using exactly the same algorithm as is already used in the FactSage software to calculate full equilibrium diagrams. This procedure has been described in detail elsewhere [6,7] and will only be briefly outlined here.

As a direct consequence of the LAPR, all phase boundaries on any single-valued full equilibrium or paraequilibrium phase diagram section are Zero Phase Fraction (ZPF) lines [6,7,10]. There is a ZPF line associated with each phase. On one side of its ZPF line the phase appears, while on the other side it does not. For example, the line *abc* in figure 1 is the ZPF line for the BCC phase and the line *abcd* in figure 3 is the ZPF line for the FCC phase.

Since all single-valued full equilibrium or paraequilibrium phase diagram sections obey the same geometrical rules, one general algorithm can be used to calculate any phase diagram section thermodynamically. At any point on a diagram the equilibrium, or paraequilibrium, state of the system can be calculated by minimizing the Gibbs energy in the case of full equilibrium or, in the case of paraequilibrium, by minimizing the Gibbs energy subject to constraints as will be described in Section 5. Along its ZPF line a phase is just present but in zero amount. To calculate any phase diagram section, the program first scans around the edges of the diagram to find the compositions of the ends of all ZPF lines. Then, starting at one end of a ZPF line it follows and draws the line by moving incrementally across the diagram, always keeping the phase just on the verge of appearing. Should a ZPF line not intersect any edge of the diagram it will be discovered by the program while it is drawing one of the other ZPF lines. When the ZPF lines of all phases have been drawn the diagram is complete. This procedure can be used to calculate any single-valued full equilibrium or paraequilibrium phase diagram regardless of the axis variables and constants of the diagram. No knowledge of the topological rules governing the diagrams need be built into the algorithm; the correct topology results automatically. As was discussed in Section 2, certain phase boundaries may be coincident over part or all of their lengths. For example, in figure 3 the line segment *bc* is the ZPF line for both the FCC and cementite phases, while the segment *cd* is the ZPF line for both the FCC and BCC phases. These lines will thus be calculated and drawn twice by the algorithm.

5. A general algorithm for calculating a paraequilibrium phase assemblage

The Gibbs energy of a multiphase system is:

$$G = \sum_{\alpha} \sum_{k} n_k^{\alpha} \left(\mu_k^{0\alpha}(T) + RT \ln a_k^{\alpha} \right) \tag{2}$$

where a_k^{α} refers to the activity of constituent *k* in phase α, being in general a function of composition, temperature and pressure; and where n_k^{α} denotes molar amount and $\mu_k^{0\alpha}$ standard chemical potential. Minimization of the Gibbs energy, *e.g.*, for calculation of phase diagrams, conventionally requires an optimization of the non-linear *G*-function, Eq. (2), made at constant pressure and temperature, with mass balances as linear constraints and usually is performed by the Lagrange method of undetermined multipliers [11]. The mass balances are defined by using a stoichiometry matrix, the elements of which are derived from the composition of the system. The independent system components are chemical elements (or their stoichiometric associations) and the constituents (also known as "end members") of each phase are species of their linear combinations. The balance equation then reads as follows:

$$\sum_{\alpha=1}^{NP} \sum_{k=1}^{N_\alpha} c_{kj}^{\alpha} n_k^{\alpha} - b_j = 0 \qquad (j = 1, 2, \ldots, NC); \quad (n_k^{\alpha} \geq 0) \tag{3}$$

where *NC* and *NP* are the numbers of components and phases respectively. Here b_j is the molar amount of system component *j* in the closed system and c_{kj}^{α} are the coefficients of the (*N*×*NC*) stoichiometry matrix as given by the chemical formulae of the constituents which may be present in the system. The summation is made over all constituents in all phases ($N = N_\alpha + N_\beta + \cdots + N_{NP}$). The subscript *j* refers to the *j*th element or system component in the molecular formula of constituent *k*.

By using the method of Lagrange, the objective function to be minimized then becomes:

$$L = G - \sum_{j=1}^{NC} \pi_j \left[\sum_{\alpha=1}^{NP} \sum_{k=1}^{N_\alpha} c_{kj}^{\alpha} n_k^{\alpha} - b_j \right] \tag{4}$$

where π_j are the undetermined Lagrange multipliers used to include the constraints into the objective function *L*. The solution of the optimization problem then provides both the Lagrange multipliers (as chemical potentials of the components) and the equilibrium amounts of the constituents. In conventional min(*G*) calculations the summation includes all system components, but the minimization procedure may also include complementary (immaterial) conditions such as conservation of charge or surface area in cases where surface phases are considered. As a general rule, such additional constraints must not violate the original mass or energy balances of the Gibbsian system.

The use of immaterial constraints in Gibbsian calculations has been recently generalized in a method called Constrained Gibbs Energy Minimization [12,13]. This method is straightforward for partitionless transformations described, for example, by Hillert [2] but has also been applied for composition-constrained systems by Kozeschnik [3,14]. A partitionless transformation is

defined as one involving transforming from $\alpha \rightarrow \beta$ without change in composition between the reactant (parent) phase and the product phase. This leads to a condition where the use of composition-based constraints in the Lagrangian problem will give the respective results in min(G) calculations for any number of restricted phases and constituents [3]. The choice of reference component is arbitrary; however as the discussion above is focussed on steel solidification, it is convenient to select iron as such. Then, the amounts of all metal components will remain equal to the molar ratios as referenced to Fe in the original parent phase:

$$\frac{\text{Fe}}{\text{Me}} = \frac{\sum_k c_{kFe}^{\alpha} n_k^{\alpha}}{\sum_k c_{kMe}^{\alpha} n_k^{\alpha}} = Y_{Me} \qquad (\alpha = 1, 2, \ldots, NP) \qquad (5)$$

where the summations are over all constituents of each paraequilibrium phase in the system and Fe and Me refer to molar amounts of iron and an immobile (metal) component, respectively, in the parent phase. Eq. (5) may be written as a mass balance:

$$\sum_k Y_{Me} c_{kMe}^{\alpha} n_k^{\alpha} - \sum_k c_{kFe}^{\alpha} n_k^{\alpha} = 0 \qquad (6)$$

Thus the conservation of the Fe/Me ratio requires that each constituent include a new virtual system component, *m*, which provides this particular constraint. From Eqs. (3) and (6), the matrix element of the additional virtual component *m* fulfilling this condition is

$$c_{k,m}^{\alpha} = Y_{Me} c_{kMe}^{\alpha} - c_{kFe}^{\alpha} \qquad (7)$$

and from condition (6), the total amount of the virtual component in each phase is zero; *i.e.*, its presence will conserve the desired mass ratio of the metal components in each of the paraequilibrium phases but will not affect the overall mass balance of the system. With several immobile components and several paraequilibrium phases, a separate virtual component is needed for each combination. When the number of phases (*NP*) and the number of immobile components (*M*) is larger than two, the number of required virtual constraint components is given by (*NP*-1)(*M*-1). Of the phases permitted in the Gibbs energy minimization, the paraequilibrium solution phases must contain all diffusing elements and pure stoichiometric phases must contain diffusing elements only.

It may be noted that, while in the Gibbsian calculation the chemical potential of each phase constituent at equilibrium is given as a linear combination of the product $c_{kj}\pi_j$ summed over all system components [11, 12], Eq. (7) together with the respective Lagrange multipliers leads to the condition

$$u_{Fe}^{\alpha}\mu_{Fe}^{\alpha} + \sum_{Me} u_{Me}^{\alpha}\mu_{Me}^{\alpha} = u_{Fe}^{\beta}\mu_{Fe}^{\beta} + \sum_{Me} u_{Me}^{\beta}\mu_{Me}^{\beta} \qquad (8)$$

in the paraequilibrium system, where $u_{Me} \equiv$ Me/Z where Z is the total molar amount of non-diffusing components. As stated by Hillert [2], the new phase-independent quantity is thus defined as the weighted average of the chemical potential of iron and other (substitutional) metals, as if they had formed a new element in the system. The diffusing (interstitial) components are not constrained and will reach equilibrium by equality of their chemical potentials in all phases.

It can further be noted that there is nothing fundamentally unique about component 'Fe' in the formulation. The constraints could be calculated equally well with respect to some other immobile component; generally *M*-1 constraints for each constrained phase for *M* immobile components. As described above, the use of this technique also allows for the extension to minimum Gibbs energy phase diagram calculations, for which there are no diffusing elements.

Acknowledgements

The authors are indebted to Prof. Christopher Bale for his assistance and advice. Financial assistance from the Natural Sciences and Engineering Research Council of Canada is gratefully acknowledged.

References

[1] A. Hultgren, Trans. ASM, 39 (1947) 915.

[2] M. Hillert, Phase Equilibria, Phase Diagrams and Phase Transformations – Their Thermodynamic Basis, 2nd ed., Cambridge Univ. Press, Cambridge UK, 2008, pp 311-315.

[3] E. Kozeschnik, J.M. Vitek, Calphad 24 (2000) 495-502.

[4] C.W. Bale, E. Bélisle, P. Chartrand, S.A. Decterov, G. Eriksson, K. Hack, I.-H. Jung, Y.-B. Kang, J. Melançon, A.D. Pelton, C. Robelin, S. Petersen, Calphad 33 (2009) 295-311; <www.factsage.com>.

[5] L.S. Palatnik, A.I. Landau, Zh, Fiz. Khim., 30 (1956) 2399.

[6] A.D. Pelton in: G. Kostorz (Ed.), Phase Transformations in Materials, Wiley-VCH, Weinheim, Germany, 2001, pp 1-80.

[7] A.D. Pelton in: Physical Metallurgy 5th ed, Elsevier, In press.

[8] N. Saunders, A.P. Miodownik, J. Mater. Res., 1 (1986) 38.

[9] P.J. Spencer, Z. Metallkunde, 92 (2001) 1145-1150.

[10] H. Gupta, J.E. Morral, H. Nowotny, Scripta Metall., 20 (1986) 889.

[11] W.R. Smith, R.W. Missen: Chemical reaction equilibrium analysis: theory and algorithms, Krieger, Malabar, Florida, 1991.

[12] P. Koukkari, R. Pajarre, Calphad, 30 (2006) 18.

[13] P. Koukkari, R., Pajarre, Pure App. Chem., 83, (2011) 1243.

[14] E. Kozeschnik, Calphad, 24, (2000) 245.

FIGURE CAPTIONS

FIGURE 1. Full equilibrium phase diagram section of the Fe-Cr-C system showing tie-lines. Mole fraction X_C versus mole fraction X_{Cr} at constant T = 1140^{o}C. (Formation of graphite suppressed).

FIGURE 2. Full equilibrium phase diagram section of the Fe-Cr-C system. Molar ratio C/(Fe+Cr) versus T at constant molar ratio Cr/(Fe+Cr) = 0.04. (Formation of graphite suppressed).

FIGURE 3. Paraequilibrium phase diagram section of the Fe-Cr-C system when C is the only diffusing element. Molar ratio C/(Fe+Cr) versus T at constant molar ratio Cr/(Fe+Cr) = 0.04. (Formation of graphite suppressed).

FIGURE 4. Paraequilibrium phase diagram section of the Fe-Cr-C system when C is the only diffusing element. Mole fraction X_C versus T at constant mole fraction X_{Cr} = 0.04. (Formation of graphite suppressed).

FIGURE 5. Paraequilibrium phase diagram section of the Fe-Cr-C system when C is the only diffusing element. Molar ratio C/(Fe+Cr) versus molar ratio Cr/(Fe+Cr) at constant T = 775^{o}C. Tie-lines are shown. (Formation of graphite suppressed).

FIGURE 6. Paraequilibrium phase diagram section of the Fe-Cr-C system when C is the only diffusing element. Mole fraction X_C versus mole fraction X_{Cr} at constant T = 775^{o}C. Tie-lines are not horizontal. (Formation of graphite suppressed).

FIGURE 7. Paraequilibrium phase diagram section of the Fe-Cr-C system when C is the only diffusing element. Molar ratio Cr/(Fe+Cr) versus T at constant molar ratio C/(Fe+Cr) = 0.05. (Formation of graphite suppressed).

FIGURE 8. Paraequilibrium phase diagram section of the Fe-Cr-C-N system when C and N are the only diffusing elements. Molar ratio Cr/(Fe+Cr) versus T at constant molar ratios C/(Fe+Cr) = N/(Fe+Cr) = 0.02. (Formation of graphite suppressed).

FIGURE 9. Paraequilibrium phase diagram section of the Fe-Cr-Ni-Mn-Mo-C system when C is the only diffusing element. Molar ratio C/Z, where Z = (Fe + Cr + Ni + Mn + Mo), versus T at constant molar ratios Cr/Z = Ni/Z = Mn/Z = Mo/Z = 0.01. (Formation of graphite suppressed).

FIGURE 10. Paraequilibrium phase diagram section of the Fe-Cr-Ni-Mn-C system when C is the only diffusing element. Molar ratio Cr/Z, where Z = (Fe + Cr + Ni + Mn), versus T at constant molar ratios C/Z = 0.04, Ni/Z = Mn/Z = 0.02. (Formation of graphite suppressed).

FIGURE 11. Full equilibrium phase diagram of the Ni-Cr system. Mole fraction Cr versus T.

FIGURE 12. Minimum Gibbs energy phase diagram of the Ni-Cr system. Mole fraction Cr versus *T*.

FIGURE 13. Minimum Gibbs energy phase diagram section of the Fe-Ni-Cr system at 600^{o}C.

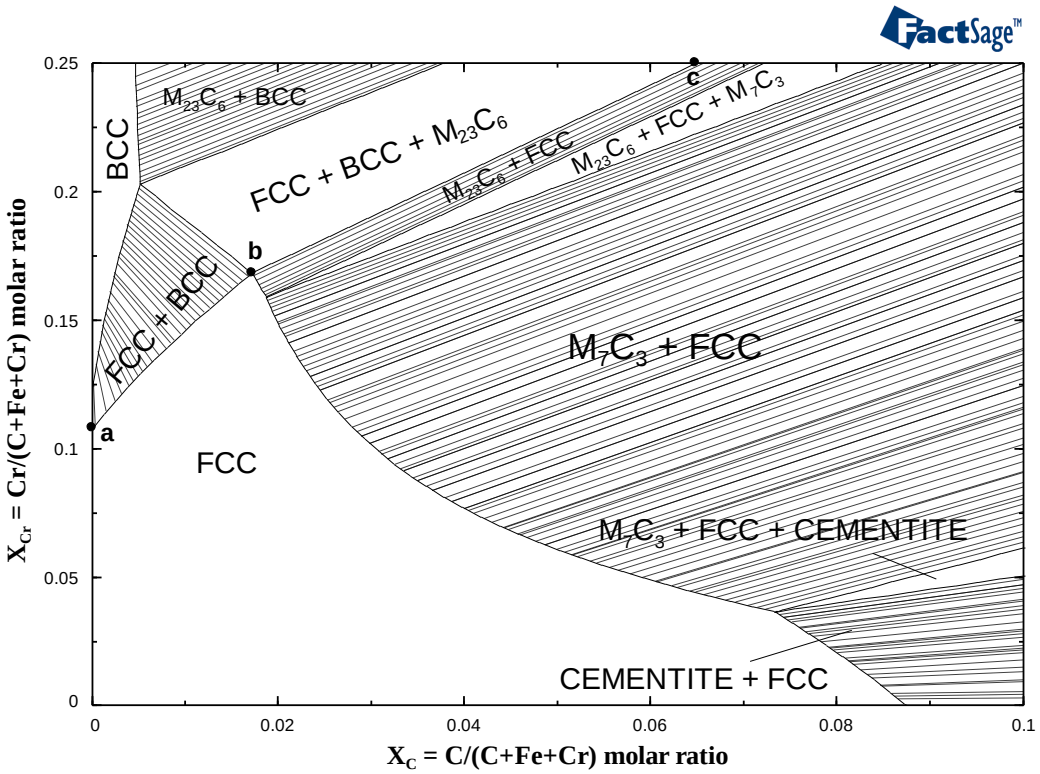

FIGURE 1. Full equilibrium phase diagram section of the Fe-Cr-C system showing tie-lines. Mole fraction X_C versus mole fraction X_{Cr} at constant T = 1140°C. (Formation of graphite suppressed).

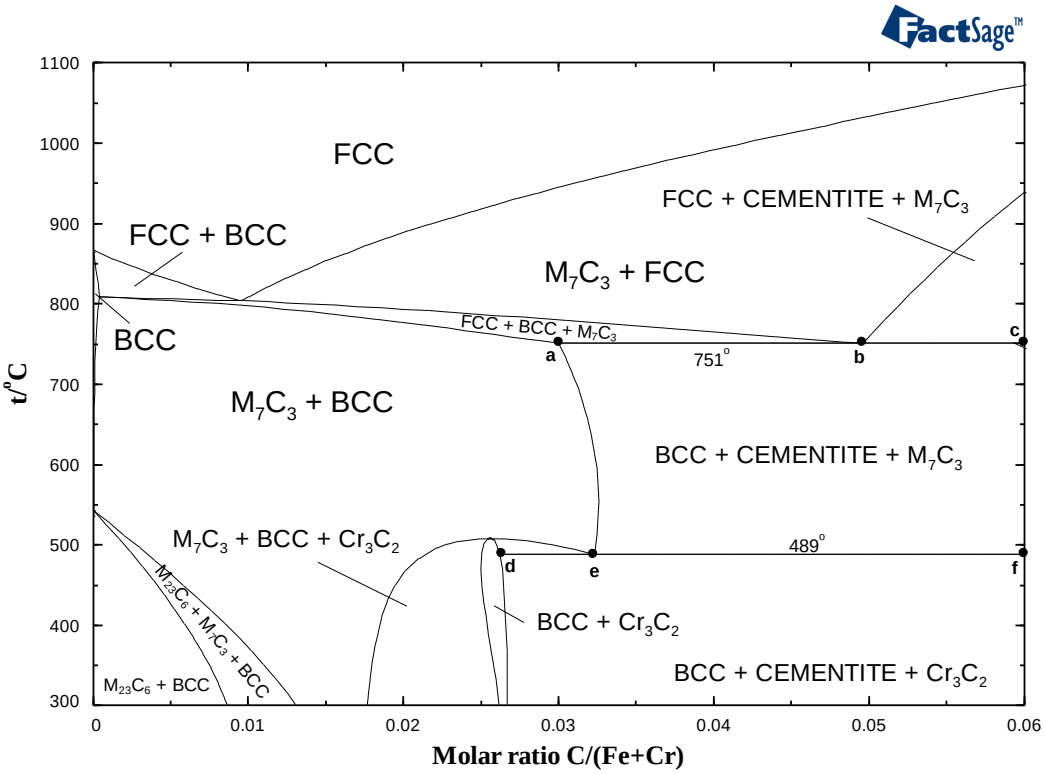

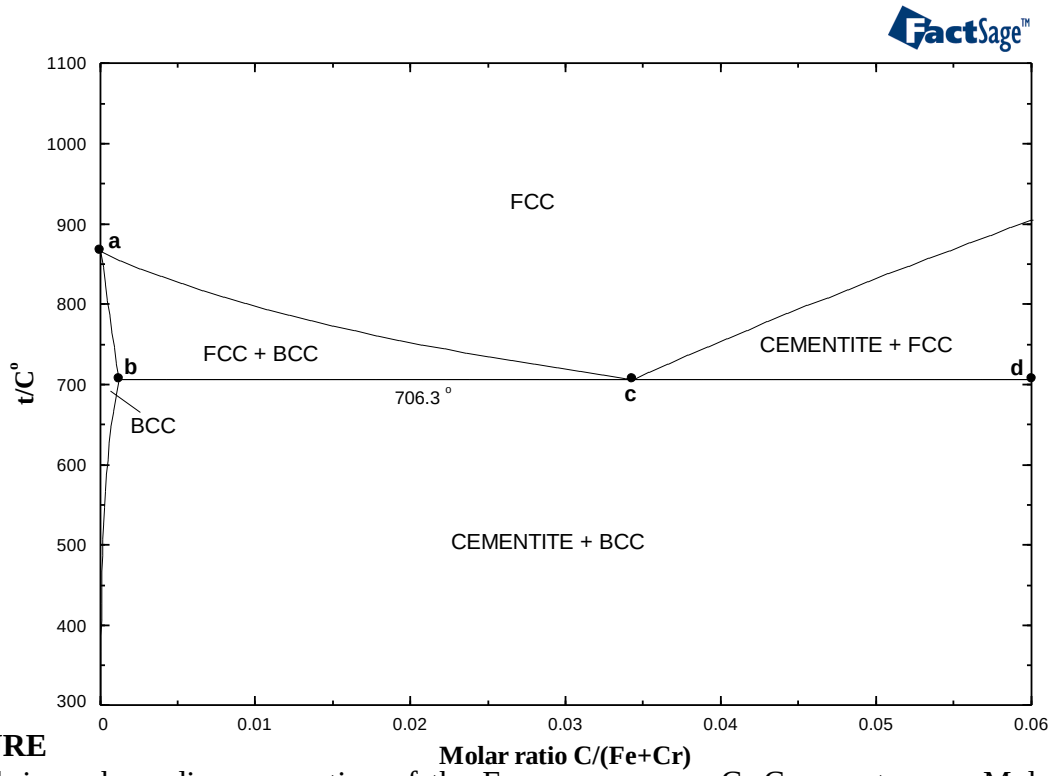

FIGURE 2. Full equilibrium phase diagram section of the Fe-Cr-C system. Molar ratio C/(Fe+Cr) versus T at constant molar ratio Cr/(Fe+Cr) = 0.04. (Formation of graphite suppressed).

FIGURE 3. Paraequilibrium phase diagram section of the Fe-Cr-C system when C is the only diffusing element. Molar ratio C/(Fe+Cr) versus *T* at constant molar ratio Cr/(Fe+Cr) = 0.04. (Formation of graphite suppressed).

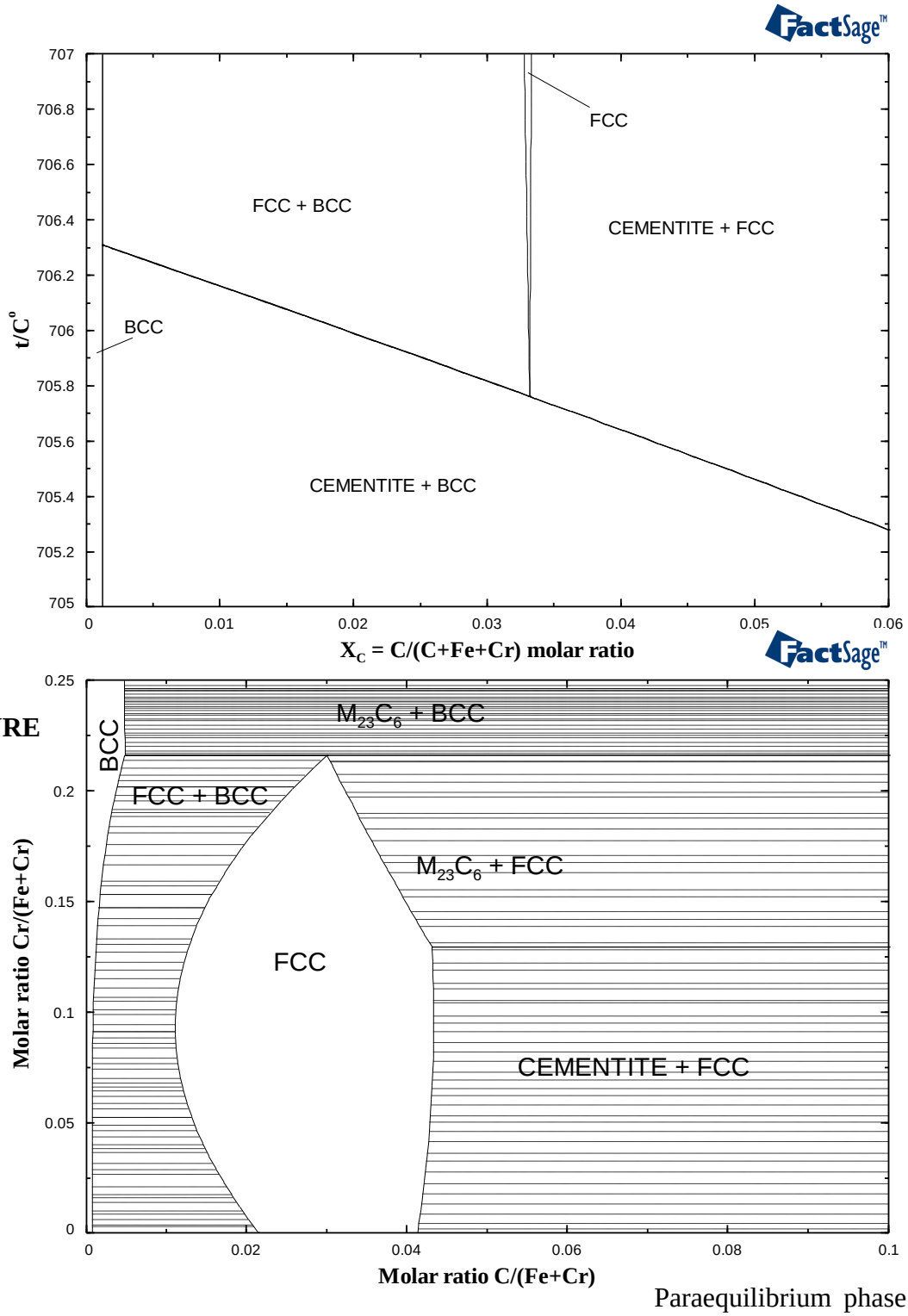

FIGURE 4. Paraequilibrium phase diagram section of the Fe-Cr-C system when C is the only diffusing element. Mole fraction X_C versus T at constant mole fraction X_{Cr} = 0.04. (Formation of graphite suppressed).

FIGURE 5. Paraequilibrium phase diagram section of the Fe-Cr-C system when C is the only diffusing element. Molar ratio C/(Fe+Cr) versus molar ratio Cr/(Fe+Cr) at constant T = 775°C. Tie-lines are shown. (Formation of graphite suppressed).

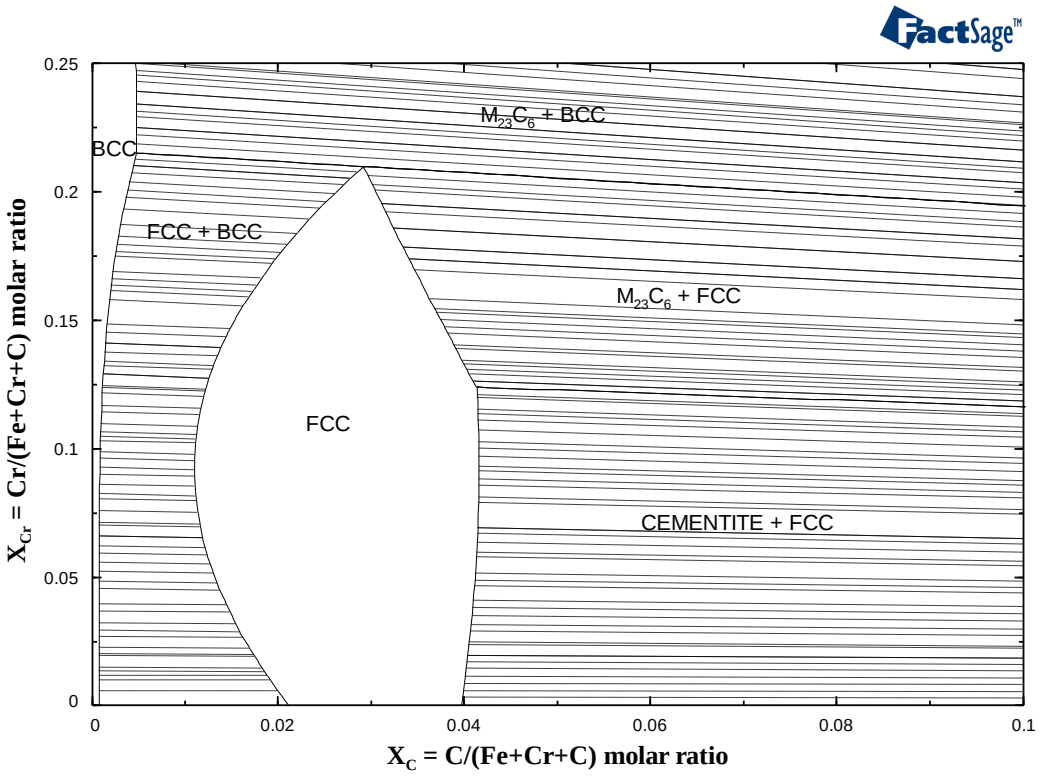

FIGURE 6. Paraequilibrium phase diagram section of the Fe-Cr-C system when C is the only diffusing element. Mole fraction X_C versus mole fraction X_{Cr} at constant T = 775°C. Tie-lines are not horizontal. (Formation of graphite suppressed).

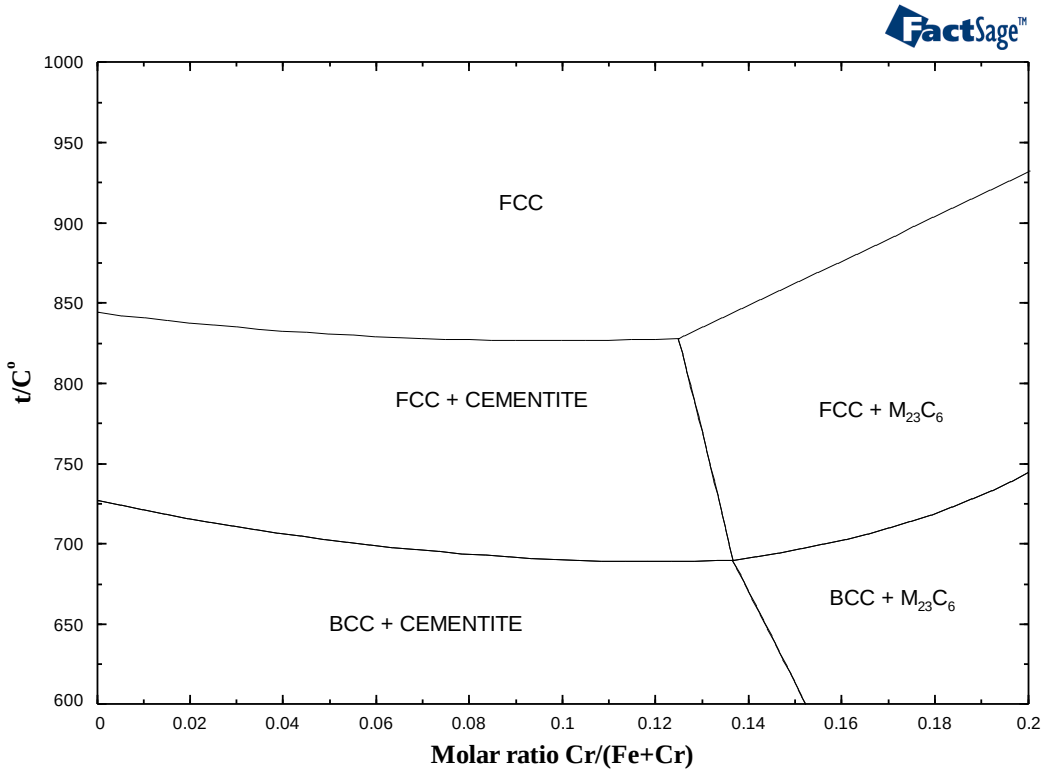

FIGURE 7. Paraequilibrium phase diagram section of the Fe-Cr-C system when C is the only diffusing element. Molar ratio Cr/(Fe+Cr) versus *T* at constant molar ratio C/(Fe+Cr) = 0.05. (Formation of graphite suppressed).

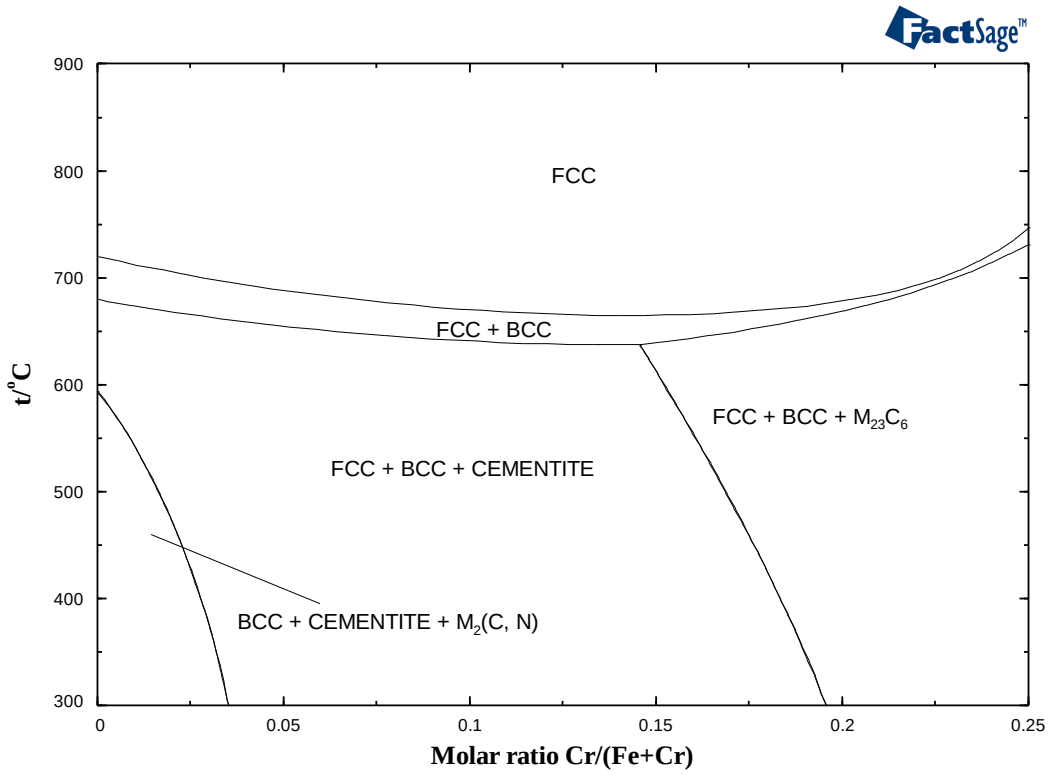

FIGURE 8. Paraequilibrium phase diagram section of the Fe-Cr-C-N system when C and N are the only diffusing elements. Molar ratio Cr/(Fe+Cr) versus *T* at constant molar ratios C/(Fe+Cr) = N/(Fe+Cr) = 0.02. (Formation of graphite suppressed).

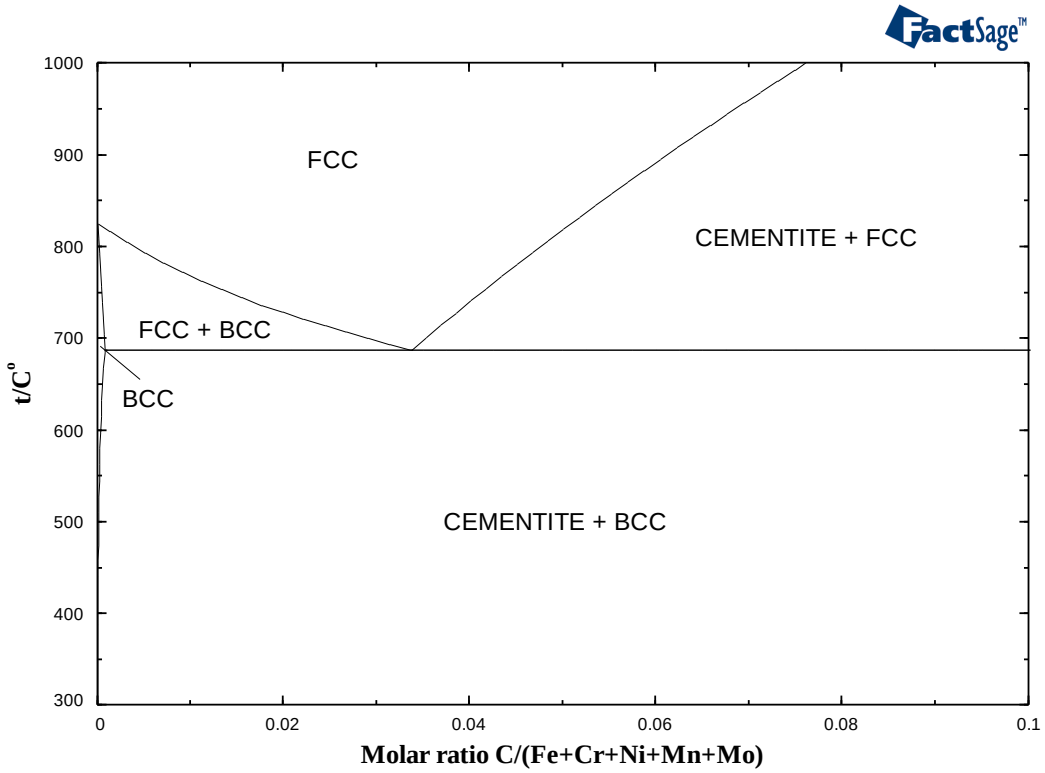

FIGURE 9. Paraequilibrium phase diagram section of the Fe-Cr-Ni-Mn-Mo-C system when C is the only diffusing element. Molar ratio C/Z, where Z = (Fe + Cr + Ni + Mn + Mo), versus *T* at constant molar ratios Cr/Z = Ni/Z = Mn/Z = Mo/Z = 0.01. (Formation of graphite suppressed).

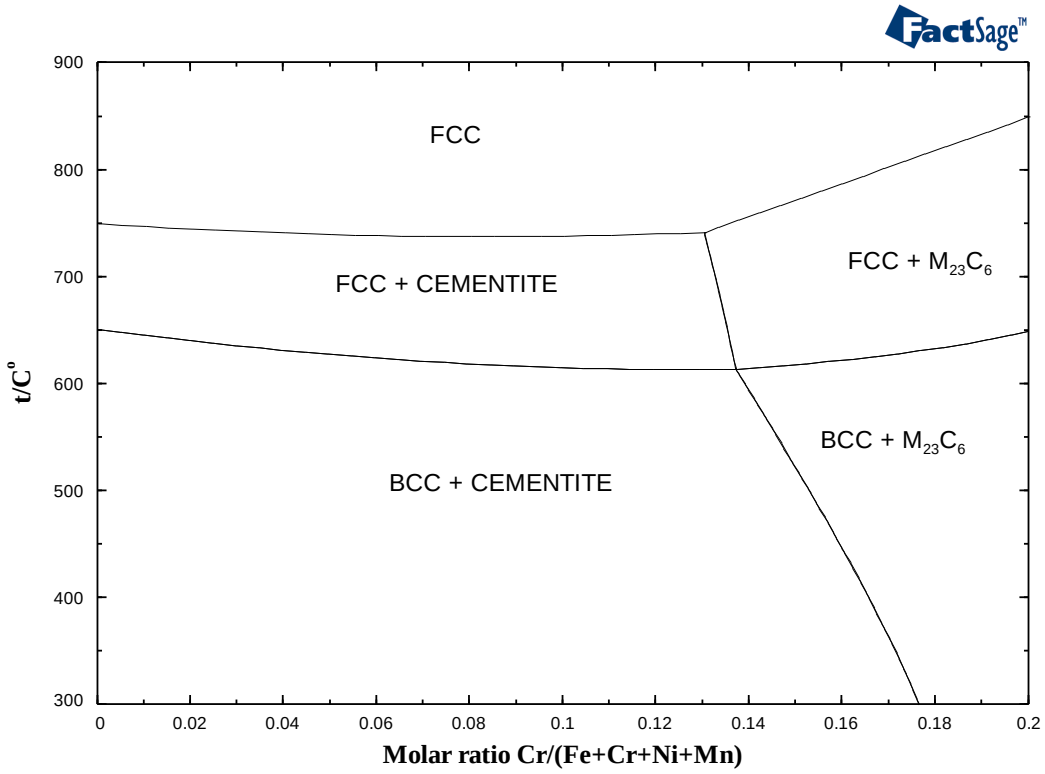

FIGURE 10. Paraequilibrium phase diagram section of the Fe-Cr-Ni-Mn-C system when C is the only diffusing element. Molar ratio Cr/Z, where Z = (Fe + Cr + Ni + Mn), versus *T* at constant molar ratios C/Z = 0.04, Ni/Z = Mn/Z = 0.02. (Formation of graphite suppressed).

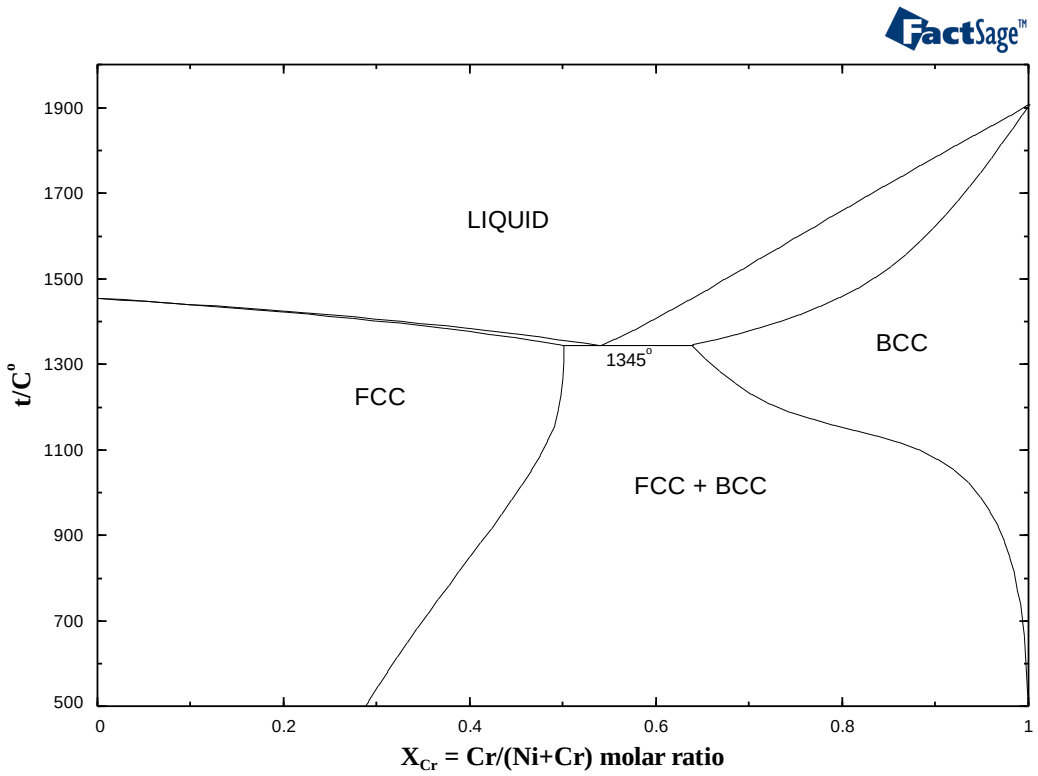

FIGURE 11. Full equilibrium phase diagram of the Ni-Cr system. Mole fraction Cr versus *T*.

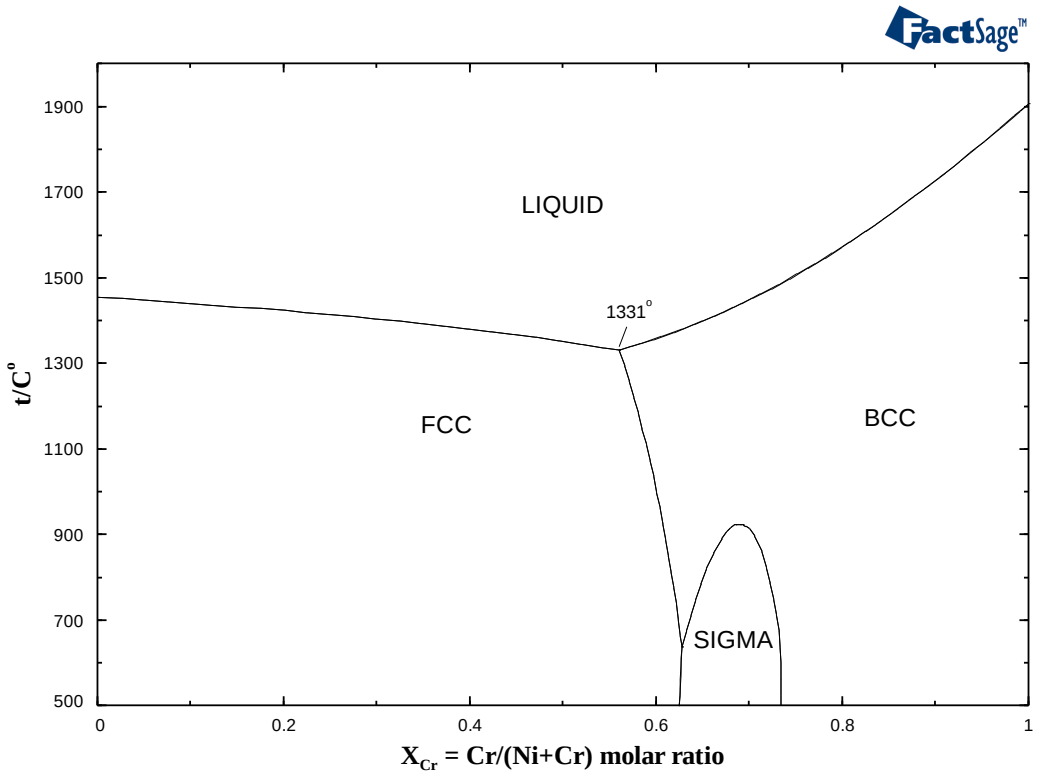

FIGURE 12. Minimum Gibbs energy phase diagram of the Ni-Cr system. Mole fraction Cr versus *T*.

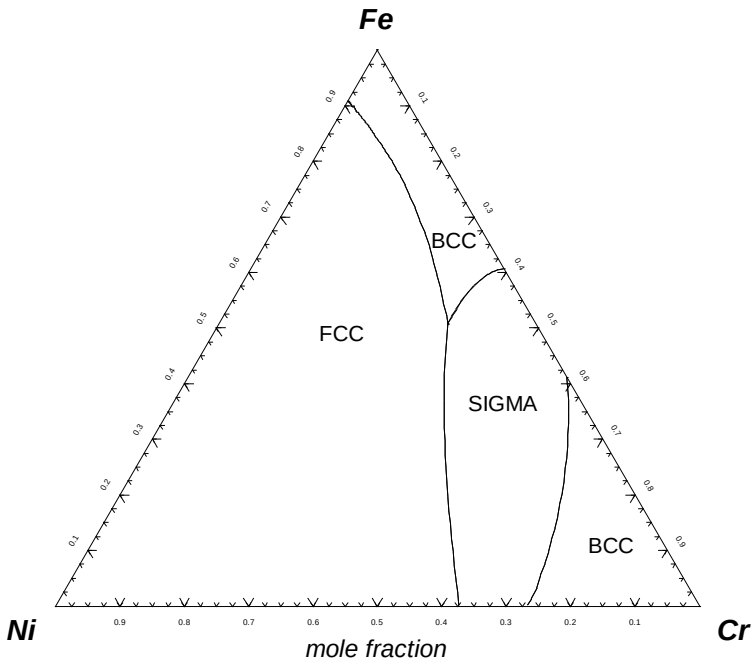

FIGURE 13. Minimum Gibbs energy phase diagram section of the Fe-Ni-Cr system at 600^{o}C.